Accepted Manuscript

Spectroelectrochemical detection of specifically adsorbed cyanurate anions at gold electrodes with (111) orientation in contact with cyanate and cyanuric acid neutral solutions

William Cheuquepán, Antonio Rodes, José M. Orts, Juan M. Feliu

Please cite this article as: William Cheuquepán, Antonio Rodes, José M. Orts, Juan M. Feliu , Spectroelectrochemical detection of specifically adsorbed cyanurate anions at gold electrodes with (111) orientation in contact with cyanate and cyanuric acid neutral solutions. The address for the corresponding author was captured as affiliation for all authors. Please check if appropriate. Jeac(2017), doi: 10.1016/j.jelechem.2017.02.015

Spectroelectrochemical detection of specifically adsorbed cyanurate anions at gold electrodes with (111) orientation in contact with cyanate and cyanuric acid neutral solutions.

William Cheuquepán#, Antonio Rodes*#&, José M. Orts*#, Juan M. Feliu*#

*Departamento de Química Física and #Instituto Universitario de Electroquímica

Universidad de Alicante, Apartado 99, 03080 Alicante, SPAIN

&Corresponding autor. E-mail: Antonio.rodes@ua.es; Tel/Fax: (+34) 965909814

Abstract

The adsorption and reactivity of cyanate at Au(111) single crystal and Au(111)-25 nm thin film electrodes is studied spectroelectrochemically in sodium perchlorate solutions and compared to those of cyanuric acid ($C_3N_3O_3H_3$). From the Surface Enhanced Infrared Reflection Absorption spectra obtained under Attenuated Total Reflection conditions (ATR-SEIRAS) it can be concluded that adsorbed cyanate species predominate at the electrode surface for low cyanate concentrations. However, for cyanate concentrations above 1 mM, the similarity of the ATR-SEIRA spectra with those obtained in cyanuric acid containing solutions indicates that some species coming from cyanuric acid is formed and adsorbed at the (111) gold surface sites as the result of an electroless trimerization reaction. Taking into account the results of Density Functional Theory (DFT) calculations, the experimental voltammetric and ATR-SEIRAS results agree with the formation of adlayers of specifically adsorbed triketo-monocyanurate species that adsorb perpendicular to the electrode surface.

**Keywords:** Au(111); cyanuric acid; ATR-SEIRAS; DFT; cyanate

1. Introduction.

Cyanate is a simple anion species whose adsorption and oxidation have been studied in the past at various electrode materials [1-11]. Published papers include in situ spectroscopic studies (either infrared [1-11] or Raman [7]) dealing with the identification of the adsorbed species formed from cyanate-containing solutions as well as the corresponding cyanate oxidation products. The adsorption of cyanate was detected as a potential-dependent process as witnessed by the observation of a band around 2220 cm^{-1}, ascribed by most authors to N-bonded cyanate anions [2-6,10]. Besides, Kitamura et al. [3] and Corrigan and Weaver [4] observed both for platinum [3,4] and gold [4] electrodes a band at ca. 2260 cm^{-1} that was attributed to isocyanic acid (HNCO) molecules resulting from the protonation of cyanate anions. This latter process would be induced by the protons released upon the electrochemical oxidation of the electrode surface. Taking into account the calculated optimized adsorbate geometries, adsorption energies and vibrational harmonic frequencies obtained from DFT calculations for cyanate and related species adsorbed at gold [11], we confirmed the assignment of the adsorbate bands between 2100 and 2300 cm^{-1} to the asymmetric OCN stretch of N-bonded, specifically adsorbed isocyanate anions. The observation of absorption bands in a relatively wide spectral region agrees with the coexistence of N-bonded cyanate species with different adsorption sites (mainly top) and tilting angles. In addition, the existence of collective in-phase vibrations at relatively high cyanate coverages also contributes to the widening of the absorption bands. The calculated adsorption energies [11] for cyanic and isocyanic acid indicate that these species adsorb weakly at the studied gold surfaces and, thus, seem not to be at the origin of any of the adsorbate bands.

In the papers commented above, no bands below 1800 cm^{-1} were reported for in situ infrared spectra, which were collected under external reflection conditions [1-11], thus indicating that adsorbed cyanate was the only adsorbate formed from dissolved cyanate anions. However, in a more recent paper, we have reported the first ATR-SEIRAS study of cyanate adsorption at Au(111)-25 nm [12] that changes the picture described above. Both the strong exaltation of the

infrared absorption by adsorbates and the removal of interferences due to the bulk solvent characteristic of the ATR-SEIRAS technique [13,14] helped in the observation of new absorption bands in the range between 1800 and 1300 cm^{-1}, not detected previously in the external reflection experiments with gold single crystal electrodes [11]. These bands appear far from the typical wavenumbers for adsorbed cyanate (either adsorbed or in solution), thus suggesting the formation of new adsorbed chemical species. We proposed the formation of species derived from isocyanuric acid ($C_3N_3O_3H_3$) a trimer of isocyanic acid (HNCO) [15]. Cyanuric acid is a highly stable chemical, widely used as a stabilizer for chlorine in the treatment and maintenance of pool water. This high stability is at the origin of the difficulties found for its removal. Some electrochemical treatments (using boron-doped diamond electrodes) have been reported, however, that are successful in achieving the total mineralization of cyanuric acid [16].

The chemical behavior of cyanuric acid and its derivatives has been widely studied, including different synthetic pathways (see the review by Seifer [15] and references therein). There are different tautomeric forms compatible with this molecular species. Some discussion existed in the past regarding the nature of the most stable tautomer (either the triketo or the trienolic form, both depicted in reaction 1).

(1)

s-   triazine-2,4,6-trione   s-triazine-2,4,6-triol
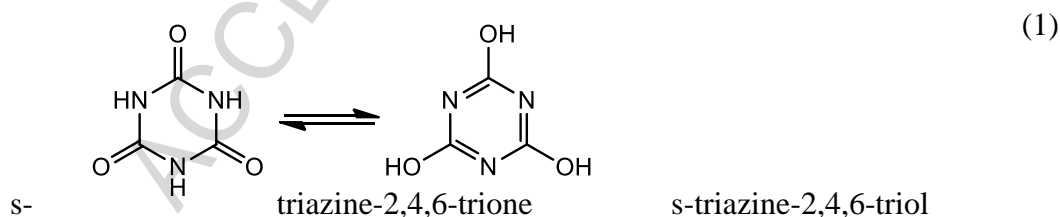
This issue is finally settled, after different theoretical and experimental studies that are discussed in detail in the paper by Revan [17]. From these works it is concluded that the triketo (trioxo) form is the most stable tautomer, both in gas-phase [17-20] and in solutions with different solvents [21]. The differences in energy found by Revan [17] (in gas phase) between the triketo form of cyanuric

acid and the other tautomers with different degrees of enolization range between 70 and 160 kJ·mol^{-1}. Another relevant property of cyanuric acid is its behavior as a weak acid (with pK_a values 6.88, 11.40 and 13.5 for the successive deprotonations [22]). According to these values, the only species that are expected to exist in significant amounts both in a sodium perchlorate solution and at the electrified interface are the undissociated acid and the monocyanurate anion ($C_3N_3O_3H_2^-$) that results from the first acid dissociation. In this anion the negative charge on the N atom is stabilized by resonance with the two neighboring carbonyl groups.

(2)
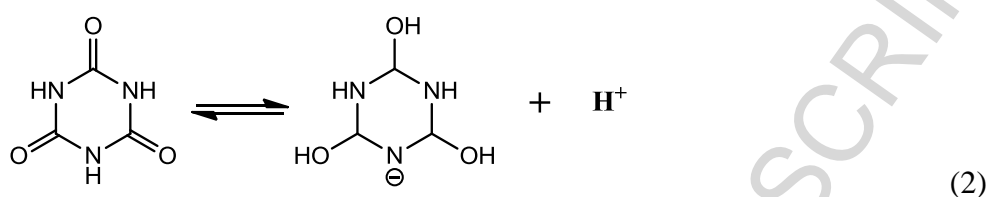
Some precedents exist regarding the study of adlayers of cyanuric acid, either alone or mixed with melamine, as these systems form well-ordered self-assembled monolayers on Au(111) [23-27]. The results of the structural characterization using STM under different conditions indicate that for most of the experimental conditions studied [23,25-27], in these adlayers the cyanuric acid molecule adsorbs weakly, parallel to the surface, forming hydrogen bond between neighbouring adsorbates that increase the stability of the adlayer. We are not aware of any published result regarding the adsorption or electrochemical behavior of cyanurate on gold electrode surfaces.

In this work, we extend our preliminary study of the adsorption and reactivity of cyanate at gold electrodes by exploring the behavior in contact with solutions having a wide range of cyanate and cyanuric acid concentration. In order to support the interpretation of the experimental results (in particular, band assignments) we have compared the in-situ ATR-SEIRA spectra recorded in these solutions with the theoretical frequencies obtained by periodic DFT calculations for the most plausible candidate structures to be adsorbed at the electrode surface. Finally, we compare also the voltammetric behavior of cyanuric acid at the (111) preferentially oriented gold thin film electrodes and Au(111) single crystal electrodes, showing the existence of characteristic features of ordered (111) domains.

2. Experimental section.

Working solutions were prepared in ultrapure water (18.2 MΩ·cm, Elga-Vivendi) by dissolving either sodium cyanate (96%, Sigma-Aldrich) or cyanuric acid (98%, Sigma-Aldrich) in a 0.08 M solution of sodium perchlorate (99.99%, Sigma-Aldrich). Deuterium oxide (99.9 atom %D, Aldrich) was used as the solvent in some experiments as received. All these solutions were deaerated with Ar (N50, Air Liquide) and maintained under an atmosphere of this gas during the experiments.

The spectroelectrochemical Pyrex glass cells used in this work are equipped with a silicon prismatic window beveled at 60º [28]. A Ag/AgCl/KCl (sat) electrode and a gold wire were used as the reference and the counter electrode, respectively. The working electrode in the ATR-SEIRAS experiments was a 25 nm-thick gold thin film fabricated by thermal evaporation on one of the faces of the silicon prism. Film deposition was carried out in the vacuum chamber of a PVD75 (Kurt J. Lesker Ltd.) coating system at a base pressure around 10^{-6}Torr. A quartz crystal microbalance was used for monitoring the deposition rate (fixed at 0.006 nm s^{-1}), and the thickness of the gold film. The surface quality of these thin films was further improved by electrochemical annealing in the spectroelectrochemical cell filled with a 10 mM CH_3COONa + 0.1 M $HClO_4$ solution [29]. Due to its preferential (111) orientation this electrode will be named along the text as Au(111)-25 nm [14]. Some voltammetric experiments were carried out with Au(111) single crystal electrodes (ca. 2 mm diameter), which were prepared from a gold wire (Alpha Aesar 99.999%) following Clavilier's method [30,31] . These electrodes were heated in a gas-oxygen flame before the experiments, cooled in air and protected with a droplet of ultrapure water [31-33].

In situ infrared experiments were carried out using a Nexus 8700 (Thermo Scientific) spectrometer equipped with a Veemax (Pike Tech.) reflectance accessory and a MCT-A detector. All the spectra were collected with a resolution of 8 cm^{-1} and are presented in absorbance units (a.u.) as – log(R/R$_o$), where R and R$_o$ represent the single beam sample and reference reflectivity spectra, respectively. Positive-going and negative-going bands correspond, respectively, to gain or loss of

species for the sample spectrum with respect to the reference spectrum. Sets of 100 interferograms were collected at different sample potentials and referred to a reference single beam spectrum collected in the working solution either before or after dosing the molecule at the indicated potential.

3. Computational details.

Geometry optimization and calculation of harmonic vibrational frequencies for the adsorbates studied (undissociated cyanuric acid and monocyanurate) were carried out using the Projector-Augmented-Wave (PAW) method [34,35] as implemented in the VASP [36-39] code (version 4.6). The density functional chosen was that proposed by Perdew, Burke and Ernzehof [40,41]. The relative energy values reported do not include the correction of zero point vibrational energy. Brillouin zone sampling used the Monkhorst-Pack [42] (3x3x1) scheme. Smearing was done with the second order method of Methfessel-Paxton [43] (sigma = 0.2 eV). The convergence criteria used were: 10^{-5} eV for electronic convergence, and 0.02 eV/angstrom for the forces on atoms.

The periodic models of the unreconstructed Au(111) surfaces were slabs of 4 metallic layers, with a (3x3) periodicity, separated by more than 12 Angstrom of vacuum. The positions of the gold nuclei (9 per layer, for a total of 36) were kept fixed at their bulk positions, without allowing relaxation. A value of 4.1748 Angstrom was used for the lattice constant, determined from the fitting to a Murnaghan equation of state. This value agrees well with experimental values reported for pure gold crystals (4.065 Angstrom) [44].

4. Experimental results.

4.1. Cyanate solutions.

Figure 1A reports stationary cyclic voltammograms obtained with a Au(111)-25 nm electrode in contact with 0.08 M sodium perchlorate solutions containing sodium cyanate with concentrations

ranging from 0.01 to 10 mM. The electrode potential was cycled between -0.55 to +0.60 V, thus excluding the potential range where cyanate anions and/or the electrode surface are oxidized. The latter process could eventually compromise the mechanical integrity of the deposited thin-film electrode whereas the study of cyanate oxidation is out of the scope of this work. The presence of cyanate in the working solution causes a significant charge contribution superimposed to the voltammetric response of the cyanate-free solution (curve a) for potentials above -0.20 V and cyanate concentrations above 0.1 mM (see curves c-e in Figure 1A). This additional charge contribution becomes higher for increasing cyanate concentrations. Note that the negative shift of the voltammetric features in Figure 1A for increasing cyanate concentrations is typical and indicative of the presence of specifically adsorbed species. It is worth pointing out that, in the explored potential region, there are no significant faradic oxidation currents that could be related to the irreversible oxidation of cyanate anions. The voltammetric profile recorded for a given cyanate concentration is similar to that reported for the Au(111) electrode [11]. In this way, a broad feature centered at 0.25 V and a peak at ca. 0.35 V can be observed in the positive-going sweep for the 10 mM solution (curve e). The presence of some extra contributions related to the presence of a certain amounts (100) and (110) sites at the surface of the gold thin film electrode cannot be excluded. A further difference with respect to the voltammetric response of Au(111) electrode [11] is the lower definition of the voltammetric features typically associated to the potential-dependent lift of the surface reconstruction typical of wide and well-ordered (111) domains. Namely, the absence of significant differences between the first (not shown) and subsequent positive sweeps after polarizing the electrode at -0.50 V indicates that the bidimensionally ordered (111) domains are narrower in the case of the gold thin film electrode.

Figure 2 shows series of potential-dependent ATR-SEIRA spectra collected for the Au(111)-25 nm electrode in contact with 0.01 (panel A), 0.10 (panel B) and 10 mM (panel C) NaOCN concentrations in 0.08 M $NaClO_4$ solutions prepared in water. These spectra are referred to the single beam spectrum collected at -0.5 V in the corresponding working solution. The spectra

7

obtained for the 0.01 mM NaOCN concentration are characterized by an absorption band at ca. 2200 cm^{-1} which is typical for the asymmetric OCN stretching of N-bonded adsorbed cyanate as previously discussed for gold single crystal electrodes [11]. This band is observed in the ATR-SEIRA spectra for cyanate concentrations as low as 0.01 mM. This is in contrast with the absence of absorption bands in the external reflection infrared spectra collected for gold single crystal electrodes for cyanate concentrations below 1 mM [11]. Note also the lack of noticeable extra currents in the cyclic voltammogram reported in Figure 1A for the Au(111)-25 nm in the 0.01 mM solution (curve b). These observations are consistent with the extreme sensitivity of the ATR-SEIRAS experiments, allowing the detection of small amounts of adsorbates with no interferences from the consumption of dissolved cyanate. The intensity of the cyanate band in the 0.01 mM solution, which appears for electrode potentials equal to or higher than 0.20 V, increases with the electrode potential up to 0.60 V, then decreasing down to zero if the electrode potential is stepped back to -0.50 V. Additional bands in the ATR-SEIRA spectra collected for the 0.01 mM solution correspond to displaced water molecules (negative-going feature at ca 1635 cm^{-1}) as well as features for coadsorbed perchlorate anions (at ca. 1100 cm^{-1}) and uncompensated infrared absorption by the silicon substrate (at ca. 1200 cm^{-1}) (not shown in Figure 2).

Thus, it can be concluded from the spectra obtained in diluted cyanate solutions that, as expected from the corresponding cyclic voltammograms, basically reversible potential-dependent adsorption-desorption processes involving cyanate anions, water molecules and perchlorate anions are taking place at the interface. However, a different picture stems from the ATR-SEIRA spectra obtained at higher cyanate concentrations. In the case of the 1 mM and 10 mM cyanate solutions (panels B and C in Figure 2, respectively) several positive-going features appear in the spectral region between 1800 and 1300 cm^{-1} that grow in parallel with the potential-dependent feature for adsorbed cyanate (observed now for potentials above -0.20 V and with a higher band intensity than in the 0.01 mM cyanate solution for a given electrode potential). Namely, small features are observed at ca. 1743, 1450 and 1396 cm^{-1} in the 1 mM solution. These features are well-marked in the 10 mM solution. In

this way, a clear-cut feature appears at ca. 1727 cm^{-1} in the spectrum collected at -0.40 V, being blue-shifted up to ca. 1740 cm^{-1} at 0.60 V. This feature is accompanied by shoulders at ca. 1781 cm^{-1} and by additional features appearing at 1654, 1446 and 1388 cm^{-1} in the spectrum collected at 0.60 V. The intensities of all these features, as well as that of the adsorbed cyanate band, decrease down to zero when the electrode potential is stepped back to -0.50 V.

Interferences from the bending modes of interfacial water on the adsorbate bands appearing between 1800 and 1300 cm^{-1} can be avoided in experiments carried out in cyanate-containing deuterium oxide solutions. Potential-dependent spectra collected in a 10 mM cyanate solution are shown in Figure 3 (panel A). As in the case of water solutions, bands for adsorbed cyanate can be seen for all the explored cyanate concentrations, with increasing band intensities as the electrode potential increases up to 0.60 V and, at a given electrode potential, for increasing cyanate concentration (not shown). Additional bands can be appreciated for cyanate concentrations equal to or higher than 1 mM. Namely, positive-going features appear in the spectra collected with the 10 mM solution (panel A in Figure 3) at ca. 1789, 1720, 1650, 1581, 1480 and 1436 cm^{-1} (all these frequency values being measured in the spectrum collected at 0.60 V) some of them showing a band frequency strongly dependent of the electrode potential. Except for the band at ca. 1581 cm^{-1}, which cannot be observed in the spectra collected in water (probably due to the interference with the negative-going band for displaced water molecules at ca. 1630 cm^{-1}), and the small feature that appears at 1330 cm^{-1} in water (not observed in the D_2O solutions), the rest of the bands between 1800 and 1300 cm^{-1} are basically the same in water and in D_2O solutions irrespective of the cyanate concentration. A small red-shift observed in deuterium oxide solutions with respect to the corresponding spectra in water can be related to the replacement of hydrogen by deuterium atoms in the corresponding adsorbates (vide infra).

4.2. Cyanuric acid solutions.

As commented above, none of the positive-going features observed between 1800 and 1300 cm^{-1} in

the spectra obtained in cyanate-containing solutions can be related to vibrational modes for adsorbed cyanate, especially those lying in the typical carbonyl region between 1600 and 1800 cm^{-1} [45]. This result points out to the formation of some other adsorbed species from cyanate anions, either dissolved or in solution, and can be tentatively rationalized by suggesting the trimerization of adsorbed cyanate, via its equilibrium with isocyanic acid, to form cyanuric acid [12]. Since this compound is a stable chemical, we have carried out spectroelectrochemical experiments in 0.08 M NaClO$_4$ solutions containing various concentrations of cyanuric acid. In this way, Figure 1B shows the cyclic voltammograms recorded with the Au(111)-25 nm electrode in a 0.08 M sodium perchlorate solution with various cyanuric acid concentrations up to 3.3 mM. As described above for the cyanate-containing solutions, these cyclic voltammograms show between -0.20 and 0.60 V an excess of charge density with respect to the blank solution. Remarkably, a small reversible spike appears at ca. 0.48 V for cyanuric concentrations higher than 0.50 mM. This feature is shifted to less positive potentials for higher cyanuric acid concentrations and recalls the typical spike observed for the Au(111) single crystal electrode in sulphuric acid solutions, which corresponds to order-disorder transitions within the adsorbed sulphate adlayer [14]. To confirm the relation between the observed peak for the Au(111)-25 nm electrode and the existence of ordered (111) domains, additional voltammetric experiments were carried out with a Au(111) single crystal electrode in sodium perchlorate solutions containing cyanuric acid up to 10 mM. As previously reported for other specifically adsorbed anions, cyclic voltammograms in the first and second voltammetric cycles are different regarding the peak potential of the features associated to the adsorption processes in the positive-going sweep, including the lift of the surface reconstruction. For the sake of comparison with voltammograms reported above for the gold thin film electrodes, we show here only the second voltammetric profile (Figure 1C), which already corresponds to the stationary behaviour and clearly shows well-marked spikes between 0.40 and 0.60 V. These spikes, which are not observed for Au(100) electrodes (not shown), appear at less positive electrode potentials and with increasing intensities as cyanuric acid concentration increases. In a first approach, and

similarly to the interpretation given in the case of the Au(111)/sulphate adlayer [14], we can tentatively ascribe this feature to order-disorder transitions within the adsorbed layer of specifically adsorbed cyanurate anions formed in the presence of cyanuric acid. As in the case of cyanate, the voltammetric behaviour observed for the (111)-oriented electrodes in the presence of cyanuric acid agrees well with the existence of reversible, specific anion adsorption-desorption processes with no indications of the existence of any irreversible faradic process.

In preliminary ATR-SEIRAS experiments with Au(111)-25 nm electrodes in contact with cyanuric acid we restricted our discussion to the spectra collected during a potentiostatic dosing experiment at 0.20 V of cyanuric acid (up to a concentration of 0.01 mM) [11]. Some time-dependent spectra collected under these conditions can be compared in Figure 4 with those recorded when dosing was done at -0.50 V. The observed positive-going bands appearing after dosing at 0.20 V (panel B), which are similar to those detected in the cyanate-containing solutions at high cyanate concentration (see Figure 2), are not observed for dosing at -0.50 V (panel A). However, and for both sets of spectra, some negative-going bands can be observed in the water stretching (around 3500 cm^{-1}) and water bending (around 1600 cm^{-1}) regions that can be related to the displacement of interfacial water molecules as a consequence of the formation of an adsorbed adlayer. In the spectra collected at -0.50 and 0.20 V there seems not to be a positive counterpart for short times after dosing, thus suggesting the eventual formation of infrared inactive adsorbates. According to the surface selection rule for SEIRAS [46], this is consistent with the formation of species for which the dynamic dipole of the main vibrational modes are parallel to the electrode surface. It is worth noting that positive-going adsorbate bands appear in the ATR-SEIRA spectra if the electrode potential is stepped to 0.20 V after dosing at -0.50 V (see below). However, no bands are observed in such an experiment when the working solution was replaced potentiostatically by a cyanuric acid-free 0.08 M sodium perchlorate solution before the potential step. This result indicates that the adsorbed species eventually adsorbed at -0.20 V would be only weakly bonded to the electrode surface.

The potential-dependent ATR-SEIRA spectra collected for several cyanuric acid concentrations

after dosing at -0.50 V are reported in Figure 5. In the corresponding experiments, spectra collected at potentials above -0.50 V are referred to the single beam spectrum collected at this latter electrode potential in the presence of cyanuric acid. For a 0.01 mM solution, the spectra in Figure 5 (panel A) show positive absorption bands that appear at ca. 1731-1739 cm^{-1}(with a shoulder at 1785 cm^{-1}), 1654, 1438 and 1400 cm^{-1}. For the 1 and 10 mM solutions (panels B and C in figure 5) these bands become more intense and a new band appears clearly at 1581 cm^{-1}. It is worth noting that the shoulder at 1785 cm^{-1} in panel A appears as an intense band at ca. 1793 cm^{-1} in panels B and C. The potential-dependent behavior of the adsorbate bands in Figure 5 (appearing at lower potentials as the cyanuric acid concentration is increased) is parallel to the negative shift of the voltammetric features observed in Figures 1B and C. This trend is similar to that observed in the cyanate-containing solutions when comparing voltammograms in Figure 1A and ATR-SEIRA spectra in Figure 2. In this respect, it is worth noting that adsorbate bands appear at potentials well below the potential of zero charge of the Au(111) electrode in bare neutral solutions [47] as expected from the existence of specific adsorption processes.

No absorbance bands are observed at ca. 2200 cm^{-1} in the spectra reported in Figure 5 that could be ascribed to adsorbed cyanate, irrespective of the cyanuric acid concentration. However, the observed bands appear at nearly the same frequency as the features between 1800 and 1300 cm^{-1} described above for the 10 mM cyanate solution. Only some small features appearing at ca. 1480 and 1330 cm^{-1} in Figure 2 have apparently no equivalence in the spectra shown in Figure 5. The ATR-SEIRAS experiments for the cyanuric acid solution have also been carried out using deuterium oxide as the solvent. The potential-dependent spectra collected for the 10 mM solution are shown in Figure 3 (panel B) where they can be compared to those described above for the 10 mM cyanate solution in the same solvent. As mentioned above when describing the ATR-SEIRA spectra collected in the cyanate-containing solutions, the adsorbate bands observed in the cyanuric acid solutions are basically the same in water and in D$_2$O solution irrespective of the cyanuric acid concentration in the range 0.01 to 10 mM. Band frequency shifts related to the eventual

12

replacement of the hydrogen atoms in the adsorbates by deuterium are relatively small. This behavior can be understood in the light of the band assignments derived from the DFT calculations described below.

5. Computational results and discussion.

The optimized geometries and relative stability found for the undissociated cyanuric acid (triketo form) adsorbed on model Au(111) surfaces are shown in Figure 6 and Table 1, respectively. The most stable adsorption geometry (Fig. 6A) has the molecular plane parallel to the metal surface, while in the case of the other optimized geometries (structures B, C and D in Fig. 6), the molecular plane is perpendicular to the metal. In structure B the molecular plane is located just above of one surface dense atomic row, with two oxygen atoms and the N-H bond approximately above top sites. The structures C and D are misaligned by 30º from the dense rows. In structure C the nitrogen atom is bonded on top of a gold atom, and the two oxygens are nearly above bridge sites. In structure D, the bonding is through the oxygens located at top positions, with the nitrogen located above a bridge position. For all the four structures, the shortest distances to the metal atoms (around 0.4 nm) are much longer than the typical ones in chemisorption systems. This clearly indicates that irrespective of the orientation of the undissociated acid, its interaction with the surface is weak, typical of a physisorption system. Only the three less favourable structures (B, C and D) are susceptible of being eventually detected in our spectroscopic experiments, as a consequence of the surface selection rule [46]. The conclusion that undissociated triketo cyanuric acid interacts weakly with the Au(111) surface is in agreement with previous theoretical and experimental results [24,26,27].

Figure 7 shows the optimized geometries found for the monocyanurate anion adsorbed on the Au(111) model surface with different surface coordination. The structures A-C correspond to the triketo species. Their relative adsorption energies, referred to the most stable adsorbate structure found, are given in Table 2. In these structures, the molecular plane is oriented perpendicular to the

solid surface, and bonding to the metal involves the deprotonated N atom and the oxygen atoms of the two carbonyl groups in alpha positions. For the most stable coordination (structure A in Fig. 7) the molecular plane is aligned along the direction of the surface dense atomic rows, and the three atoms bound to the metal lie in positions nearly above top sites. In the other two triketo cases the molecular plane is misaligned by 30º with respect to the metal dense rows (that is, aligned with the sqrt3 direction). In structure B of Fig. 7 the adsorbate is bonded to the metal through the N atom on a top position, with the oxygen atoms located above bridge sites, but with O-Au distances too long for a strong chemical bond. Finally, in structure C of Fig. 7, the less stable among these three, there are two Au-O bonds, and the N is located approximately above a bridge site. These adsorbate structures differ from the most stable one by 8.4 and 11 kJ mol^{-1} (these are rather modest values, although still higher than the average thermal energy at room temperature, that amounts to around 2.5 kJ mol^{-1} at 300K).

In figure 7 we have also included two adsorbate structures (D and E) having one carbonyl group enolized. Tautomer D is bonded to the metal only through the nitrogen atom and the oxygen of the non-enolized vicinal oxo group. The energy of this structure is substantially higher (+73.4 kJ mol^{-1}) than for the most stable adsorbed cyanurate (structure A in Fig. 7). On the other hand, tautomer E despite keeping the tridentate adsorption geometry, is even less stable (+93,5 kJ·mol^{-1} with respect to structure A of adsorbed cyanurate). This confirms that the adsorbed enolized cyanurate species are also significantly less stable than the adsorbed keto forms, and are not likely to be present in the adlayer. Some other enolized tautomer adsorbate configurations studied (not included in this report) showed unidentate bonding to the gold surface and were even less stable than the structures reported here.

Table 3 summarizes the calculated harmonic frequency values (and their corresponding normal mode assignments) obtained for the optimized structures of monocyanurate shown in Figure 7. These values can be compared in the same table with the experimental frequencies measured at 0.60 V in the 10 mM cyanate and cyanuric acid solutions in water. Only the main contributions to the

complex combined modes for non-deuterated systems have been reported. We have also included the frequencies for the most stable triketo adsorption geometry, at full saturation coverage ($\theta=1/3$, one cyanurate per three gold surface atoms). Within the uncertainty margins typical of the experimental measurements (a resolution of 8 cm^{-1}) and taking into account the typical errors of the calculated frequencies (in average around 2-3% of the frequency values), there is a good agreement between the experimental values and those obtained for the three adsorption geometries found for the triketo-monocyanurate (structures A, B and C in Figure 7). The calculated frequencies obtained for the respective deuterated compounds have slightly lower values (by 5 to 15 cm^{-1}) that for the light isotopomer, in agreement with the experimental observations. This small shift is consistent with the small contribution of hydrogen (or deuterium) atoms to the complex modes related to each calculated frequency.

Most of the calculated frequencies obtained for the monoenolic cyanurate (structure D in figure 7) do not differ much from those of the triketo form. However, the value of 1577 cm^{-1} calculated for structure D is in clear disagreement with the experimental value (1646 cm^{-1} in cyanuric acid solution without cyanate). In the case of enolic cyanate structure E various calculated frequencies differ significantly from the experimental ones, in addition to the lack of vibrations in the carbonyl frequency range (1700-1800 cm^{-1}). If we take into account both the discrepancies in frequencies, and the much lower stability of the enolic forms (which was already known for cyanuric acid in gas and solution phases), of adsorbed cyanurate, we can conclude that the observed experimental behaviour is best explained by the presence of a monolayer of specifically adsorbed cyanurate.

The last column in Table 3 corresponds to the calculated harmonic frequencies obtained for a full monolayer (1 cyanurate per 3 surface gold atoms) of the most stable adsorption geometry of the triketo monocyanurate (structure A). This was modelled with a (3x3) simulation cell which is identical to the other cases, but contains a total of three adsorbate species. This allows to test and ilustrate the effect that the attainment of high coverage values can have in the development of collective vibration modes that can modify the vibration frequency values [48,49]. In particular, the

in-phase movement of identical adsorbates in neighbouring adsorption sites gives rise to an increase of the vibrational frequencies, than in some cases can be as significant as 50 cm^{-1}. This provides a physically meaningful explanation for the band found experimentally around 1780-1790 cm^{-1}, whose intensity growths steadily with increasing coverage during an excursion to more positive potentials. For those modes with two frequency values, the higher one corresponds to the in-phase collective vibration mode and the lower value corresponds to the out-of-phase movement.

It can be pointed out that the experimental spectra obtained in the presence of cyanate anions in solution (Figures 2 A-C and 3A) show some small features not observed in the cyanuric acid-containing solution (Figures 3B, 4 and 5). We have not tried to interpret these features but they could be tentatively attributed to the presence of cyanate anions either coadsorbed or in the immediate vicinity of the cyanurate adlayer, that could have some effect on the vibrational frequencies as a consequence of the formation of hydrogen bonds with the adsorbed cyanurate species or with the interfacial water molecules that partially hydrate the adsorbates. As indicated above, the rest of the experimental frequencies agree well with the harmonic calculated values for adsorbed triketo monocyanurate. Again, and due to the nature of the functional groups in the cyanurate adsorbates, the formation of hydrogen bonds within the cyanurate adlayer is expected. This can give rise to some shifts of the calculated frequencies that would improve the agreement with the experimental values in the cyanuric acid solutions. A complete theoretical analysis of these effects would involve a very important computational cost and is out of the scope of this paper.

6. Conclusions.

Spectroelectrochemical and theoretical results reported in this work have shed some light on the adsorption and reactivity behaviour of gold electrodes in contact with cyanate-containing neutral solutions. Whereas voltammetric results indicate the existence of reversible anion-like adsorption-desorption processes at potentials below the onset of cyanate electrooxidation, in situ ATR-SEIRAS experiments carried out with Au(111)-25 nm thin film electrodes have shown that the nature of the

adsorbed species strongly depends on the cyanate concentration. For low cyanate concentrations (below 1 mM) the observed adsorbate bands between 2100-2250 cm^{-1} reflect the formation of N-bonded cyanate anions, just as previously reported from external reflection infrared spectroscopy experiments both for polyoriented and single crystal gold electrodes. However, for cyanate concentrations higher than 1 mM, the ATR-SEIRA spectra show additional adsorbate bands between 1800 and 1300 cm^{-1} not previously observed in external reflection experiments due both to their limited surface sensitivity and to interferences by solvent vibrational modes. The observed new bands can be understood by assuming the coexistence of adsorbed cyanate with other adsorbates being formed from cyanate (either adsorbed or in solution). The characteristic band frequencies of some of the observed features (namely, those between 1800 and 1600 cm^{-1}) strongly suggest the presence of carbonyl groups such as those existing in the triketo form of cyanuric acid. This species can be considered as a trimer of isocyanic acid, the latter molecules being in equilibrium with cyanate anions.

$$3 \, NCO^- + 3 \, H^+ \leftrightarrow 3HNCO \rightarrow H_3C_3N_3O_3 \, (ads) \tag{3}$$
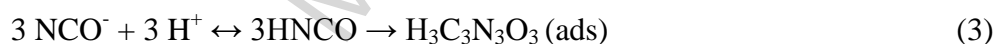
The formation of adsorbed cianuric acid (or one of its deprotonated forms) is further supported by the spectroelectrochemical experiments carried out with the Au(111)-25 nm electrode in the cyanuric acid solutions. Voltammetric profiles obtained under these conditions are similar to those recorded in the cyanate solution. Additional features appear in this voltammetric curves between 0.40 and 0.60 V, depending on the cyanuric acid concentration, that can be tentatively related to specific surface processes undergone by the adlayers of cyanuric acid (or cyanurate) formed at the ordered (111) bidimensional domains. This conclusion is corroborated by the observation of similar features in the voltammetric curves obtained with Au(111) single crystal electrodes. The ATR-SEIRA spectra collected in solutions containing low concentrations of cyanuric acid show adsorbate bands which are similar to those observed between 1800 and 1300 cm^{-1} in the cyanate-containing solutions. For higher cyanuric acid concentrations, the intensity of the bands increases significantly, especially when attaining very positive electrode potentials, where higher anion coverage values are

expected.

Comparison of the experimental band frequencies with those obtained from DFT calculations for various geometries (all perpendicular to the surface) of adsorbed monocyanurate (including triketo and monoenolic tautomeric forms) leads to the conclusion that the best explanation for the ensemble of voltammetric and IR experimental results is the existence of an adlayer formed by triketo monocyanurate species. In addition, this allows the interpretation of the blueshifting of the carbonyl signal as due to in-phase collective vibrational modes when attaining high local coverage values.

No positive-going adsorbate bands can be detected in the ATR-SEIRA spectra when dosing cyanuric acid at low potentials (-0.50 V). However negative-going water bands in the spectra collected at short times during cyanuric acid dosing experiments suggest the displacement of water molecules by an infrared-inactive weakly adsorbed species that could be tentatively identified as cyanuric acid molecules adsorbed in a configuration parallel to the metal surface. This interpretation is consistent with DFT calculations that indicate that cyanuric acid adsorbs weakly with the most stable adsorption geometry having the molecular plane parallel to the metal surface and with the shortest distances to the metal atoms being much longer than the typical ones in chemisorption systems.

Once again, the combination of high-quality voltammetry using well-defined electrode surfaces, high-sensitive in-situ IR measurements made possible by the use of the ATR-SEIRAS technique, together with the theoretical analysis by DFT calculation of adsorption geometries, relative stability and vibrational frequencies of adsorbates, has shown as a very powerful way of obtaining molecular information about the interfacial composition and structure.

ACCEPTED MANUSCRIPT

FIGURE LEGENDS

Figure 1. Stationary cyclic voltammograms of (A,B) Au(111)-25nm thin-layer or (C) Au(111) single crystal electrodes in contact with 0.08 M sodium perchlorate solutions containing A) NaOCN and B,C) cyanuric acid. In all panels, curves a correspond to the blank electrolyte; b-e) with added NaOCN or cyanuric to reach concentrations equal to b) 0.01 mM ; c) 0.1 mM ; d) 1 mM and e) 10 mM in panels A and C. In panel B, cyanuric acid concentrations were b) 0.1 mM ; c) 0.5 mM ; d) 1 mM and e) 3.3 mM. Sweep rate for all curves: 50 mV·s^{-1}.

Figure 2. Series of ATR-SEIRA spectra collected with a Au(111)-25nm thin-layer electrode in contact with 0.08 M NaClO$_4$ + x mM NaOCN solutions in water. A) x=0.01 ; B) x=1 ; C) x=10.

Figure 3. Series of ATR-SEIRA spectra collected with a Au(111)-25nm thin-layer electrode in contact with 0.08 M NaClO$_4$ + (A) 10 mM NaOCN or (B) 10 mM cyanuric solutions in D$_2$O.

Figure 4. Time-dependent ATR-SEIRA spectra obtained with a Au(111)-25nm thin-layer electrode in contact with a 0.08 M NaClO$_4$ solution, after dosing cyanuric acid in amount to reach a concentration of 0.1 mM. Dosage potential: A) -0.50 V and B) 0.20 V. Spectra are referred to the single beam spectrum collected at the same potential just before the addition of the cyanuric acid.

Figure 5. Series of potential-dependent ATR-SEIRA spectra collected with a Au(111)-25nm thin-layer electrode in contact with 0.08 M NaClO$_4$ + x mM cyanuric acid solutions in water. A) x=0.01; B) x=1 ; C) x=10.

Figure 6. Calculated optimized structures of adsorbed cyanuric acid on Au(111).

Figure 7. Calculated optimized structures of adsorbed monocyanurate on Au(111).

Reference List

1. O. Hofmann, K. Doblhofer, and H. Gerischer, "*Infrared reflection-absorption measurements on emersed gold electrodes*", J. Electroanal. Chem. Interfacial Electrochem., 161 (1984) 337-344.

2. D. S. Corrigan and M. J. Weaver, "*Coverage-dependent orientation of adsorbates as probed by potential-difference infrared spectroscopy: azide, cyanate, and thiocyanate at silver electrodes*", J. Phys. Chem., 90 (1986) 5300-5306.

3. F. Kitamura, M. Takahashi, and M. Ito, "*Anodic oxidation of cyanide and cyanate ions on a platinum electrode*", Chem. Phys. Lett., 136 (1987) 62-66.

4. D. S. Corrigan and M. J. Weaver, "*Adsorption and oxidation of benzoic acid, benzoate, and cyanate at gold and platinum electrodes as probed by potential-difference infrared spectroscopy*", Langmuir, 4 (1988) 599-606.

5. D. S. Corrigan and M. J. Weaver, "*The interpretation of solution electrolyte vibrational bands in potential-difference infrared spectroscopy*", J. Electroanal. Chem., 239 (1988) 55-66.

6. J. D. Roth and M. J. Weaver, "*Potential-difference surfac infrared spectroscopy under forced hydrodynamic flow conditions : control and elimination of adsorbate solution-phase interferences*", Anal. Chem., 63 (1991) 1603-1606.

7. M. Bron and R. Holze, "*Cyanate and thiocyanate adsorption at copper and gold electrodes as probed by in situ infrared and surface-enhanced Raman spectroscopy*", J. Electroanal. Chem., 385 (1995) 105-113.

8. M. Bron and R. HOLZE, "*Polarization sensitive in situ infrared spectroscopy: the adsorption o f simple ions platinum electrodes*", Fresenius. J. Anal. Chem., 361 (1998) 694-696.

9. K. Brandt, E. Vogler, M. Parthenopoulos, and K. Wandelt, "*In situ and ex situ FTIR characterization of a cyanate adlayer on Cu(111)*", J. Electroanal. Chem., 570 (2004) 47-53.

10. O. Yepez and B. R. Scharifker, "*Mechanistic pathways during oxidation of cyanate on platinum single crystal faces*", Electrochim. Acta, 50 (2005) 1423-1429.

11. W. Cheuquepan, J. M. Orts, A. Rodes, and J. M. Feliu, "*DFT and spectroelectrochemical study of cyanate adsorption on gold single crystal electrodes in neutral medium*", J. Electroanal. Chem., in press (2016) Electronic version: DOI: 10.1016/j.jelechem.2016.10.11.

12. W. Cheuquepan, A. Rodes, J. M. Orts, and J. M. Feliu, "*Formation of cyanuric acid from cyanate adsorbed at gold electrodes*", Electrochem. Commun., in press (2016) Electronic version: DOI: 10.1016/j.elecom.2016.11.005.

13. M. Osawa, "*Dynamic processes in electrochemical reactions studied by surface-enhanced infrared absorption spectroscopy (SEIRAS)*", Bull. Chem. Soc. Jpn., 70 (1997) 2861-2880.

14. T. Wandlowski, K. Ataka, S. Pronkin, and D. Diesing, "*Surface enhanced infrared spectroscopy-Au(1 1 1-20 nm)/sulphuric acid - new aspects and challenges*", Electrochim. Acta, 49 (2004) 1233-1247.

15. G. B. Seifer, "*Cyanuric Acid and Cyanurates*", Russ. J. Coord. Chem., 28 (2002) 301-324.

16. N. Oturan, E. Brillas, and M. A. Oturan, "*Unprecedented total mineralization of atrazine and cyanuric acid by anodic oxidation and electro-Fenton with a boron-doped diamond anode*", Environ. Chem. Lett., 10 (2012) 165-170.

17. I. Reva, "*Comment on "Density functional theory studies on molecular structure, vibrational spectra and electronic properties of cyanuric acid"*", Spectrochim. Acta, Part A, 151 (2015) 232-236.

18. L. Perez-Manriquez, A. Cabrera, L. E. Sansores, and R. Salcedo, "*Aromaticity in cyanuric acid*", J. Mol. Model., 17 (2011) 1311-1315.

19. N. S. Babu and D. Jayaprakash, "*Density functional theory (DFT) studies of the stability of tautomers and equilibrium constants of cyanuric acid (CA) in different solvents*", J. Chem. Pharm. Res., 7 (2015) 1155-1160.

20. A. Zabardasti, "*Theoretical calculation of equilibrium constant for keto-enol tautomerism in cyanuric acid*", Chem. Heterocycl. Compd. (N. Y. , NY, U. S.), 43 (2007) 1344-1346.

21. Y. H. Jang, S. Hwang, S. B. Chang, J. Ku, and D. S. Chung, "*Acid Dissociation Constants of Melamine Derivatives from Density Functional Theory Calculations*", J. Phys. Chem. A, 113 (2009) 13036-13040.

22. *CRC Handbook of Chemistry and Physics, 89th Edition*", CRC Press, Boca Raton, FL, 2008.

23. W. Xu, M. Dong, H. Gersen, E. Rauls, S. Vazquez-Campos, M. Crego-Calama, D. N. Reinhoudt, I. Stensgaard, E. Laegsgaard, T. R. Linderoth, and F. Besenbacher, "*Cyanuric acid and melamine on Au(111): structure and energetics of hydrogen-bonded networks*", Small, 3 (2007) 854-858.

24. H. M. Zhang, Z. X. Xie, L. S. Long, H. P. Zhong, W. Zhao, B. W. Mao, X. Xu, and L. S. Zheng, "*One-Step Preparation of Large-Scale Self-Assembled Monolayers of Cyanuric Acid and Melamine Supramolecular Species on Au(111) Surfaces*", J. Phys. Chem. C, 112 (2008) 4209-4218.

25. W. Xu, M. Dong, H. Gersen, E. Rauls, S. Vazquez-Campos, M. Crego-Calama, D. N. Reinhoudt, E. Loegsgaard, I. Stensgaard, T. R. Linderoth, and F. Besenbacher, "*Influence of alkyl side chains on hydrogen-bonded molecular surface nanostructures*", Small, 4 (2008) 1620-1623.

26. S. Blankenburg, E. Rauls, and W. G. Schmidt, "*Role of Dihydrogen Bonds for the Stabilization of Self-Assembled Molecular Nanostructures*", J. Phys. Chem. C, 113 (2009) 12653-12657.

27. P. A. Staniec, L. M. A. Perdigao, B. L. Rogers, N. R. Champness, and P. H. Beton, "*Honeycomb Networks and Chiral Superstructures Formed by Cyanuric Acid and Melamine on Au(111)*", J. Phys. Chem. C, 111 (2007) 886-893.

28. J. M. Delgado, J. M. Orts, and A. Rodes, "*ATR-SEIRAS Study of the Adsorption of Acetate Anions at Chemically Deposited Silver Thin Film Electrodes*", Langmuir, 21 (2005) 8809-8816.

29. J. M. Delgado, J. M. Orts, and A. Rodes, "*A comparison between chemical and sputtering methods for preparing thin-film silver electrodes for in situ ATR-SEIRAS studies*", Electrochim. Acta, 52 (2007) 4605-4613.

30. J. Clavilier, D. Armand, S.-G. Sun, and M. Petit, "*Electrochemical adsorption behaviour of platinum stepped surfaces in sulphuric acid solutions*", J. Electroanal. Chem., 205 (1986) 267-277.

31. A. Rodes, E. Herrero, J. M. Feliu, and A. Aldaz, "*Structure sensitivity of irreversibly adsorbed tin on gold single-crys tal electrodes in acid media*", J. Chem. Soc. Faraday. Trans., 92 (1996) 3769-3776.

32. D. M. Kolb, "*Reconstruction phenomena at metal-electrolyte interfaces*", Prog. Surf. Sci., 51 (1996) 109-173.

33. A. Hamelin, "*Cyclic voltammetry at gold single-crystal surfaces .1. Behaviour at low index faces*", J. Electroanal. Chem., 407 (1996) 1-11.

34. P. E. Bloechl, "*Projector augmented-wave method*", Phys. Rev. B: Condens. Matter, 50 (1994) 17953-17979.

35. G. Kresse and D. Joubert, "*From ultrasoft pseudopotentials to the projector augmented-wave method*", Phys. Rev. B: Condens. Matter Mater. Phys., 59 (1999) 1758-1775.

36. G. Kresse and J. Hafner, "*Ab initio molecular dynamics of liquid metals*", Phys. Rev. B: Condens. Matter, 47 (1993) 558-561.

37. G. Kresse and J. Hafner, "*Ab initio molecular-dynamics simulation of the liquid-metal-amorphous-semiconductor transition in germanium*", Phys. Rev. B: Condens. Matter, 49 (1994) 14251-14269.

38. G. Kresse and J. Furthmueller, "*Efficient iterative schemes for ab initio total-energy calculations using a plane-wave basis set*", Phys. Rev. B: Condens. Matter, 54 (1996) 11169-11186.

39. G. Kresse and J. Furthmuller, "*Efficiency of ab-initio total energy calculations for metals and semiconductors using a plane-wave basis set*", Comput. Mater. Sci., 6 (1996) 15-50.

40. J. P. Perdew, K. Burke, and M. Ernzerhof, "*Generalized gradient approximation made simple*", Phys. Rev. Lett., 77 (1996) 3865-3868.

41. J. P. Perdew, K. Burke, and M. Ernzerhof, "*Generalized gradient approximation made simple. [Erratum to document cited in CA126:51093]*", Phys. Rev. Lett., 78 (1997) 1396.

42. H. J. Monkhorst and J. D. Pack, "*Special points for Brillouin-zone integrations*", Physical Review B-Condensed Matter, 13 (1976) 5188-5192.

43. M. Methfessel and A. T. Paxton, "*High-precision sampling for Brillouin-zone integration in metals*", Phys. Rev. B: Condens. Matter, 40 (1989) 3616-3621.

44. W. P. Davey, "*Precision measurements of the lattice constants of twelve common metals*", Phys. Rev., 25 (1925) 753-761.

45. G. Socrates, "*Infrared and Raman Characteristic Group Frequencies*", John Wiley & Sons, Chichester, 2001.

46. M. Osawa, K. Ataka, K. Yoshii, and Y. Nishikawa, "*Surface-enhanced Infrared Spectroscopy : the origin of the absorption enchancement and band selection rule in the infrared spectra of molecules adsorbed on fine metal particles*", Appl. Spectrosc., 47 (1993) 1497-1502.

47. A. Hamelin, T. Vitanov, E. S. Sevastyanov, and A. Popov, "*The electrochemical double layer on sp metal single crystals. The current status of data*", J. Electroanal. Chem., 145 (1983) 225-264.

48. D. Loffreda, D. Simon, and P. Sautet, "*Vibrational frequency and chemisorption site: a DFT-periodic study of NO on Pd(111) and Rh(111) surfaces*", Chem. Phys. Lett., 291 (1998) 15-23.

49. D. Curulla, A. Clotet, and J. M. Ricart, "*Adsorption of carbon monoxide on Pt{100} surfaces: dependence of the CO stretching vibrational frequency on surface coverage*", Surf. Sci., 460 (2000) 101-111.
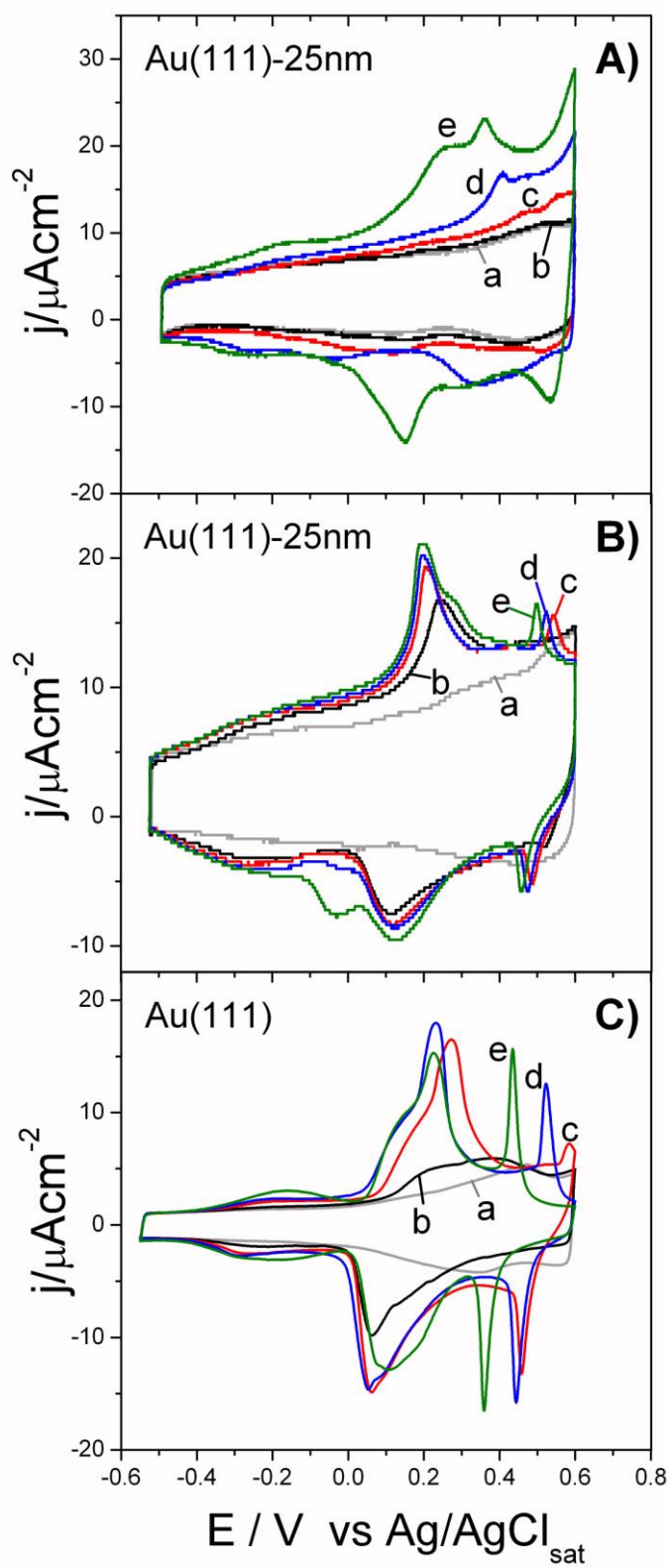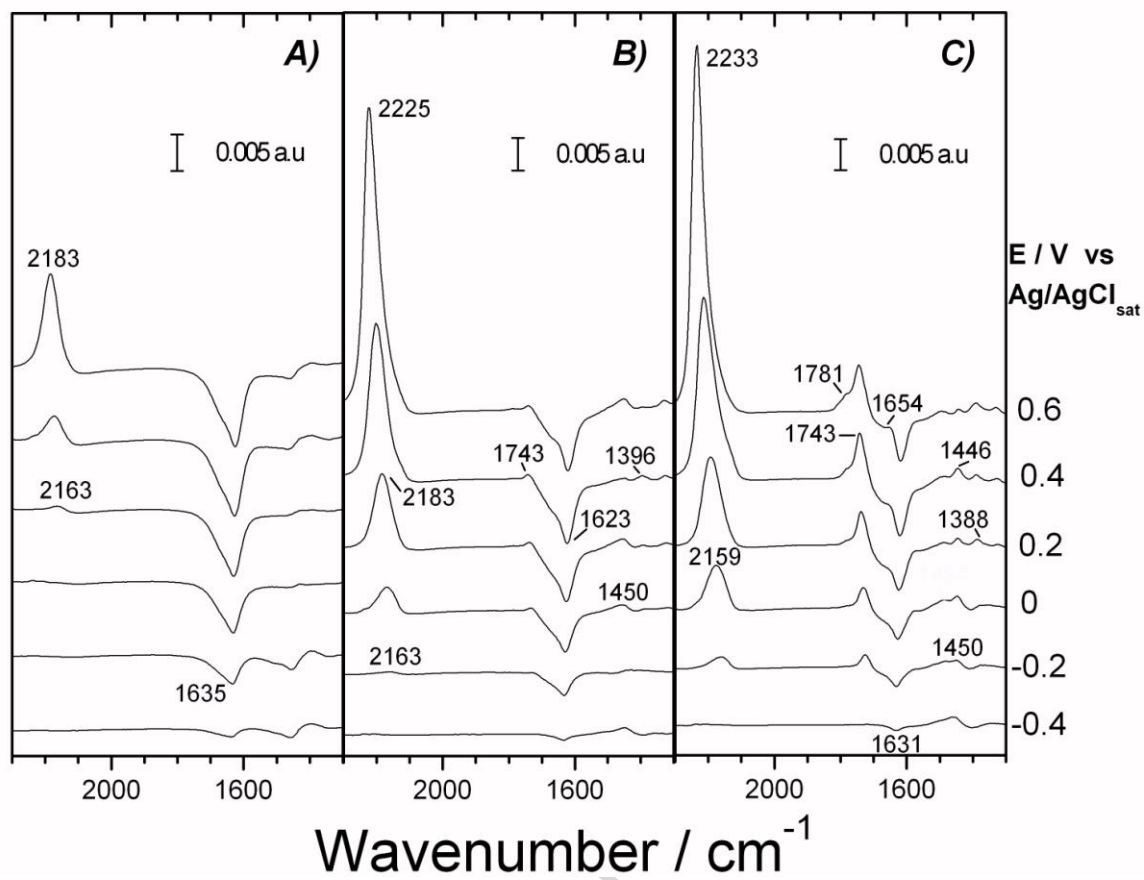
Figure 1

Au(111)-25nm

Figure 2

Figure 3
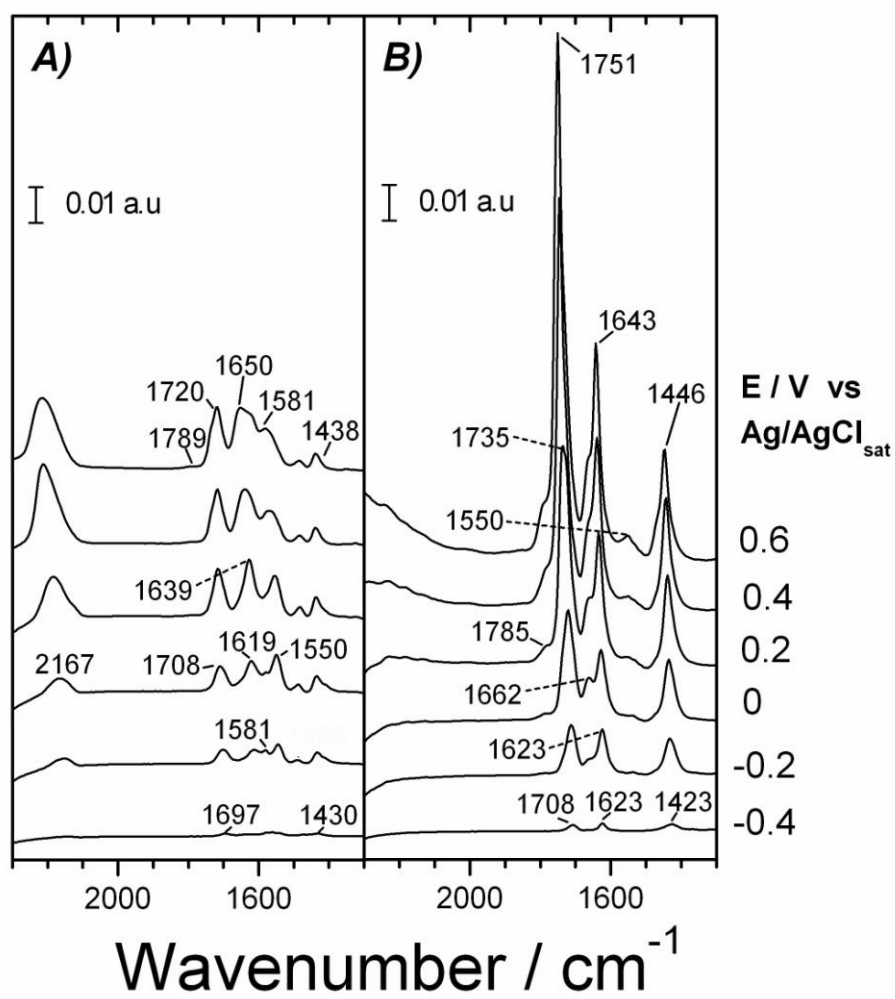
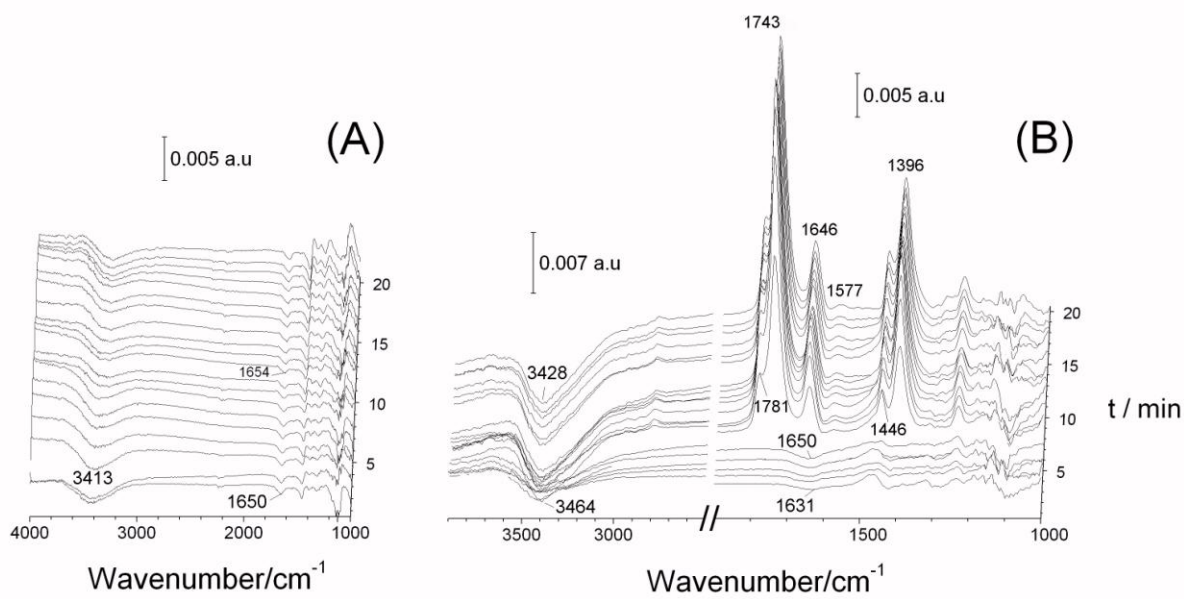Figure 4

Au(111)-25nm

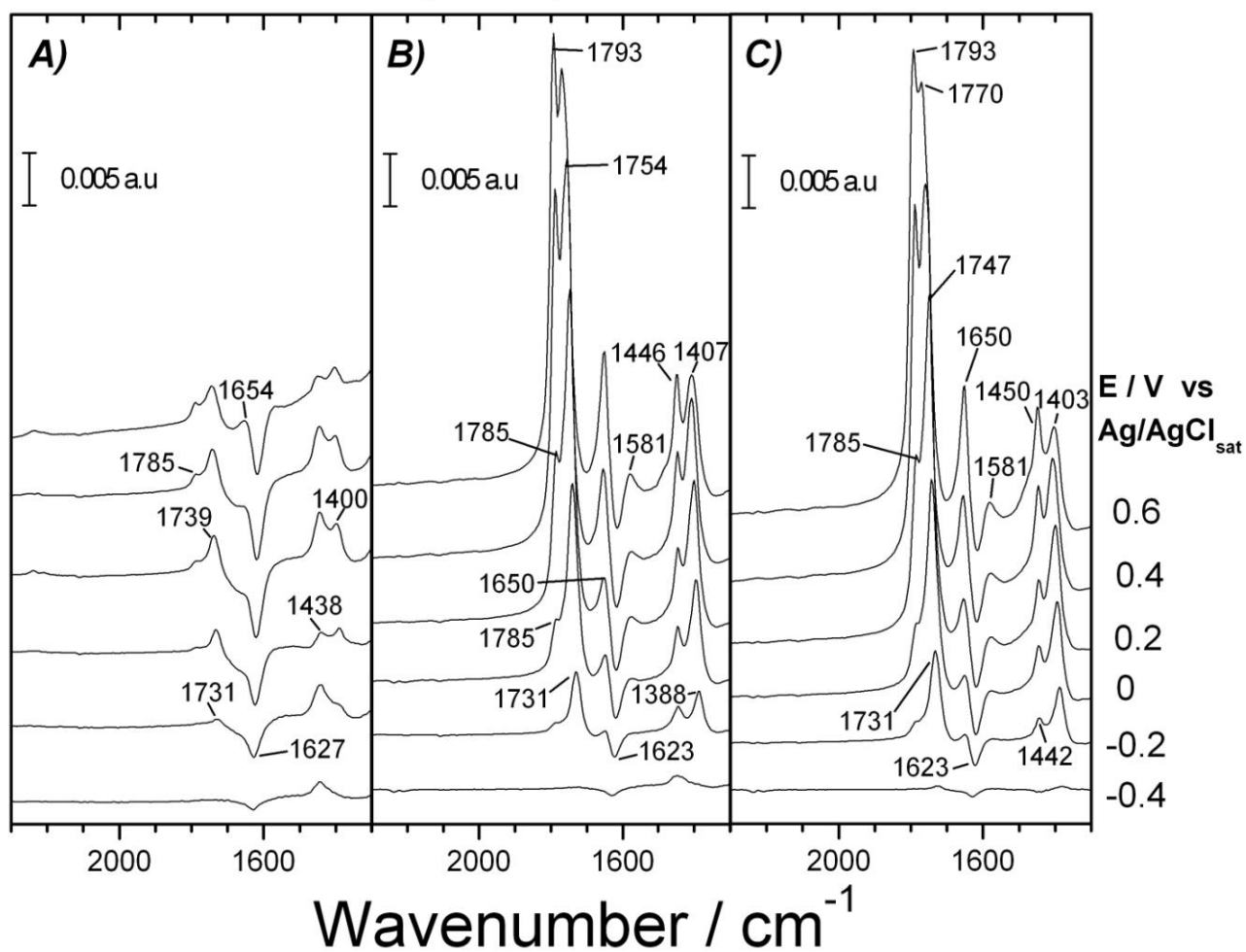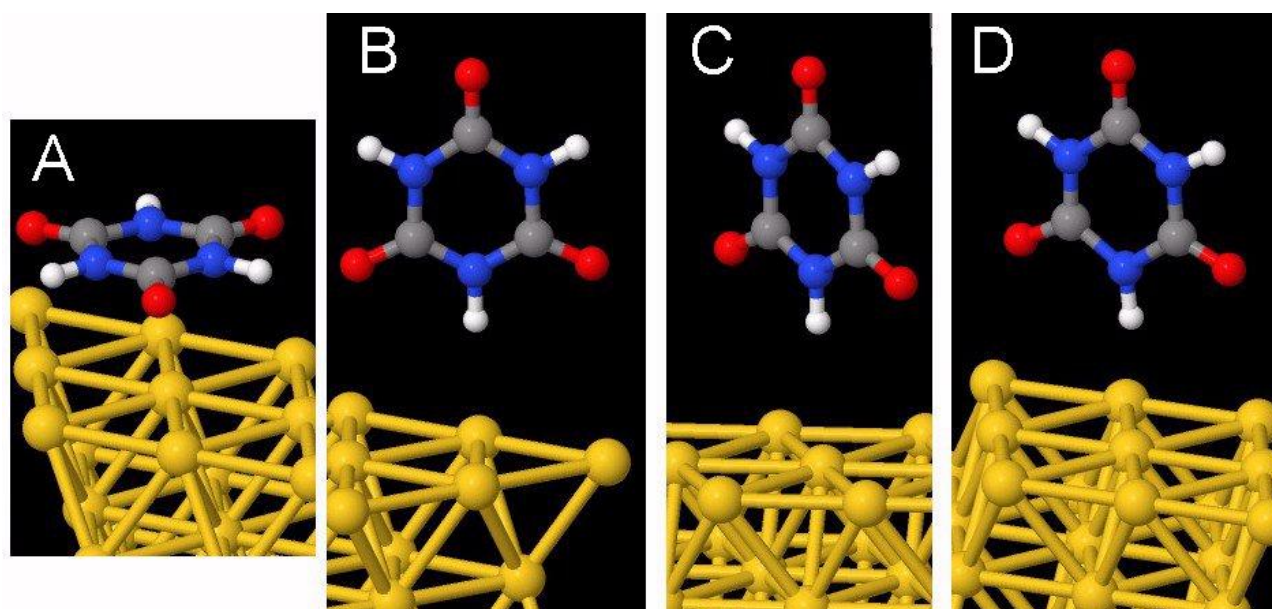Figure 5

Figure 6

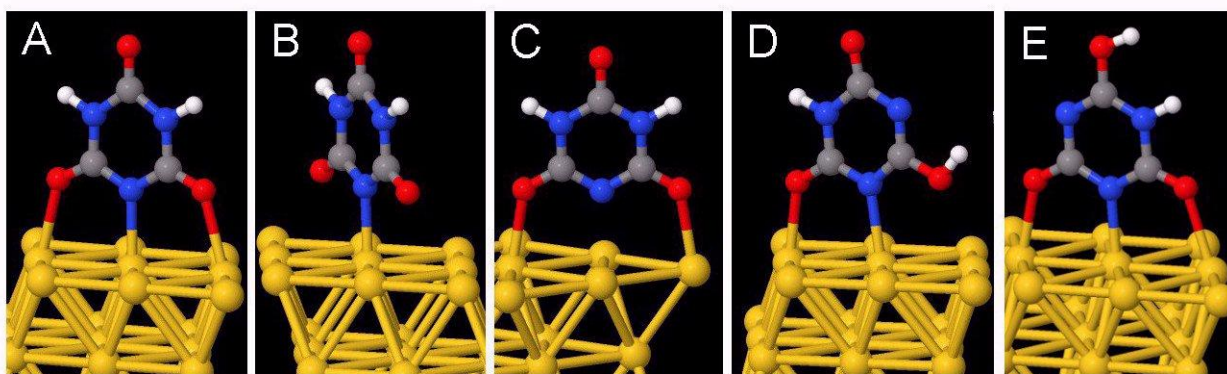Figure 7

TABLES

Table 1. Relative stability of different optimized geometries of adsorbed cyanuric acid on Au(111) model surfaces.

Structure	ΔE / kJ·mol^{-1}
A	0
B	+9.8
C	+10.4
D	+12.2

Table 2. Relative stability of different optimized geometries of adsorbed monocyanurate on

Au(111) model surfaces.

Structure	ΔE / kJ·mol^{-1}
A	0
B	+8.4
C	+10.9
D	+73.4
E	+93.5

Table 3. Experimental frequencies obtained in ATR-SEIRAS with Au(111)-25nm thin film electrodes in contact with 10 mM cyanate- and cyanuric acid-containing solutions at 0.60 V and calculated harmonic infrared frequencies corresponding to the adsorbed cyanurate structures on model Au(111) surfaces depicted in Figure 7.

Assignment	Experim. cyanate sol.	Experim. C.Acid sol.	Cyanurate Adsorbate A (θ=1/9)	Cyanurate Adsorbate B (θ=1/9)	Cyanurate Adsorbate C (θ=1/9)	Cyanurate Adsorbate D (θ=1/9)	Cyanurate Adsorbate E (θ=1/9)	Cyanurate Adsorbate A (θ=1/3)
Str CO + bend CNH	1781	1793						1810
Str CO + bend CNH	1743	1770	1769	1766	1769	1742	-	1760
Sym str OCNCO + bend CNH	1654	1650	1627	1624	1608	1577	1657, 1618	1659,1630
Asym str OCNCO + bend CNH		1581	1553	1549	1537	1544	1522	1579,1554
Asym str NCN + bend CNH	1446	1450	1416	1414	1421	1418	1461	1426,1397
Sym str NCN + bend CNH	1388	1403	1397	1391	1390	1344	1315	1406,1377

A-B: triketo cyanurate ; D-E: enolized cyanurate.

All values correspond to the non-deuterated systems.

Only the main contributions to the complex combined modes have been reported.

Highlights

1. N-bonded cyanate forms at Au(111) in the presence of low cyanate concentrations.

2. Specifically adsorbed triketo-monocyanurate is formed for higher concentrations.

3. Undissociated triketo cyanuric acid interacts weakly with the Au(111) surface.